European Journal of Medicinal Chemistry 46 (2011) 608–617

Contents lists available at ScienceDirect

European Journal of Medicinal Chemistry

journal homepage: http://www.elsevier.com/locate/ejmech

Original article

Anomalous behavior of pentacoordinate copper complexes of dimethylphenanthroline and derivatives of terpyridine ligands: Studies on DNA binding, cleavage and apoptotic activity

Subramaniyam Rajalakshmi [a], Thomas Weyhermüller [b], Allen J. Freddy [c], Hannah R. Vasanthi [c], Balachandran Unni Nair [a,*]

[a] Chemical Laboratory, Central Leather Research Institute, Council of Scientific and Industrial Research, Adyar, Chennai 600 020, India
[b] Max-Planck Institut für Bioanorganische Chemie, D-45413 Mülheim an der Ruhr, Germany
[c] Herbal and Indian Medicine Research Laboratory, Department of Biochemistry, Sri Ramachandra University, Porur, Chennai 600116, India

ARTICLE INFO

Article history:
Received 12 October 2010
Received in revised form
24 November 2010
Accepted 28 November 2010
Available online 10 December 2010

Keywords:
Copper complexes
DNA binding
Groove binder
DNA cleavage
Cytotoxicity
Apoptosis

ABSTRACT

Copper(II) complexes with substituted terpyridine ligands, namely [Cu(itpy)(dmp)]$(NO_3)_2$ (**1**) and [Cu(ptpy)(dmp)]$(NO_3)_2$ (**2**) have been synthesized and characterized. The interaction of the complexes with CT-DNA has been explored using spectroscopic techniques and viscosity. Complexes **1** and **2** bind in the grooves of DNA, interestingly **1** in the minor and **2** in the major groove. Both the complexes have been found to promote DNA cleavage; complex **1** through hydrolytic and **2** oxidative. Complexes **1** and **2** have been found to be cytotoxic and bring about apoptosis of human lung cancer cell line A549.

1. Introduction

Designs of small molecules that can mimic nucleases are of prime importance because of their potential application in medicine [1–7]. Metal complexes as DNA cleaving agents are more attractive compared to small organic compounds because of their unique spectroscopic and electrochemical properties. Ligands in the metal complexes play a major role in their binding to DNA. Large planar ligands promote intercalative binding of the metal complexes to DNA [8–13], whereas non-planar ligands and ligands not having extended planarity promote groove binding, particularly with octahedral metal complexes [14–16]. The central metal ion on the other hand, plays crucial role in the cleavage of DNA. Majority of the reported studies deal with oxidative cleavage of DNA. Many complexes of metal ions Cu(II), Ru(II), Co(III) and Cr(III) have been reported to bring about DNA cleavage in the presence of coreagent like H_2O_2 [17–20]. These complexes, in the presence of peroxide, produce hydroxyl radicals or other reactive oxygen species capable of inducing DNA strand break [21–23]. These molecules have potential application as probe for DNA structure as well as DNA and protein footprinting agent [24]. Many transition metal complexes, particularly those of Ru(II), Co(III) and Cr(III) have been shown to exhibit photonuclease activity [25–30]. There is tremendous interest in such molecules because of their application in photodynamic therapy. However, most of these molecules which cleave DNA oxidatively have severe limitations, because their activity depends on a coreagent such as an oxidizing agent or a reducing agent and this hampers their use *in-vivo*.

Mimics of endonucleases, on the other hand do not suffer from these disadvantages. Endonucleases rapidly hydrolyze DNA at physiological conditions; inspite of the fact that the phosphodiester backbone of DNA is very stable and resistive to hydrolytic cleavage [31]. As a result currently there is lot of interest in the design and synthesis of mimics of endonucleases. Some mononuclear and dinuclear complexes of Er(III), Ce(IV), Co(III), Cu(II), Fe(III) and Zn(II) have been reported to bring about efficient hydrolytic cleavage of DNA [32–36]. Hydrolytic cleavage of double stranded DNA involving phosphodiester bond offers important advantages in the cellular

* Corresponding author. Fax: +91 44 2491 1589.
E-mail address: bunair@clri.res.in (B.U. Nair).

0223-5234/$ – see front matter © 2010 Elsevier Masson SAS. All rights reserved.
doi:10.1016/j.ejmech.2010.11.041

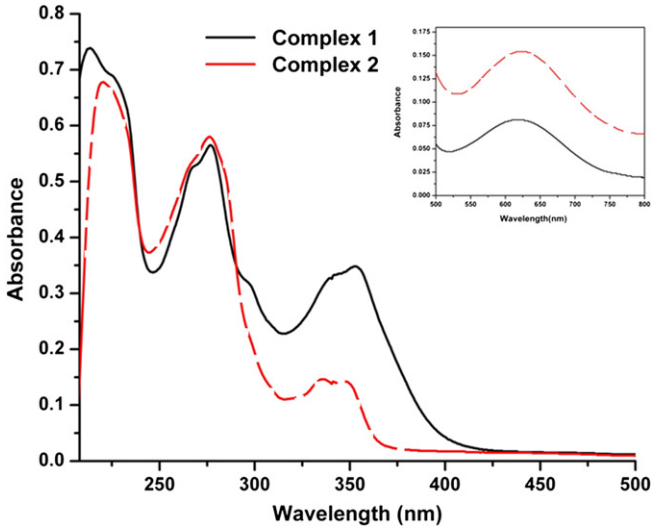

Fig. 1. Electronic spectrum of complex **1** and complex **2** in acetonitrile. Inset: visible spectra.

processes in comparison to the oxidative DNA cleavage targeted at the deoxyribose sugar moiety or the guanine base [37–40]. In this respect copper(II) complexes have attracted special attention due to their labile coordination sphere and due to the fact that copper(II) complexes can exhibit variable coordination number as well as Lewis acid–base activity for enhancing the rate of hydrolytic cleavage. A number of mononuclear copper(II) polypyridyl and mixed ligand polypyridyl complexes like $[Cu(dpq)_2(H_2O)]^{2+}$, $[Cu(dppz)_2Cl]^{+}$, $[Cu(pyrimol)Cl_2]$ and $[Cu(pbt)Br_2]$ have been reported to hydrolytically cleave DNA [41–44].

Terpyridyl and its derivatives are versatile ligands as well as prominent building blocks in both organic and inorganic supramolecular chemistry because of their π stacking ability. However, they have not attracted as much attention as bipyridyl derivatives. Terpyridine derivatives have the potential to form four, five as well as six coordinated complexes. Mixed ligand complexes of copper(II) with terpy derivatives and bipy derivatives will be interesting molecules because of the possibility of one water molecule occupying the sixth coordination site. Such molecules may be good candidates to bring about hydrolytic cleavage of DNA. The present

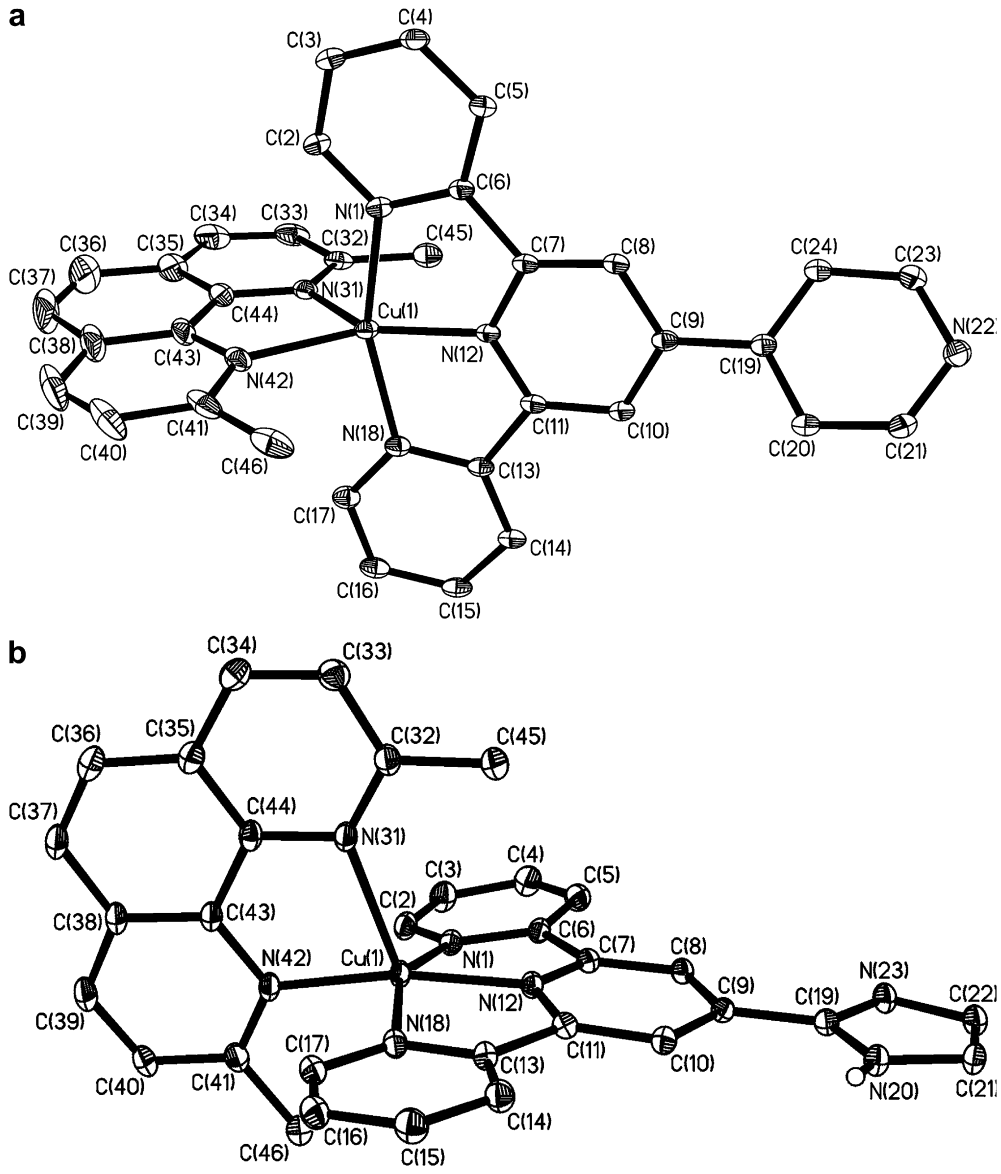

Fig. 2. (a) ORTEP diagram for complex **1**; (b) ORTEP diagram for complex **2**.

Table 1
Selected bond lengths and bond angles of complexes **1** and **2**.

Bond distances/A°		Bond angle (°)	
[Cu(itpy)(dmp)]$(NO_3)_2 \cdot 4.5H_2O$			
Cu(1)–N(12)	1.931(2)	N(12)–Cu(1)–N(42)	169.46(9)
Cu(1)–N(42)	1.980(2)	N(12)–Cu(1)–N(1)	79.58(9)
Cu(1)–N(1)	2.037(2)	N(42)–Cu(1)–N(1)	99.49(9)
Cu(1)–N(18)	2.053(2)	N(12)–Cu(1)–N(18)	79.95(8)
Cu(1)–N(31)	2.219(2)	N(42)–Cu(1)–N(18)	98.38(8)
		N(1)–Cu(1)–N(18)	156.11(8)
		N(12)–Cu(1)–N(31)	110.28(8)
		N(42)–Cu(1)–N(31)	80.21(8)
		N(1)–Cu(1)–N(31)	102.44(8)
[Cu(itpy)(dmp)]$(NO_3)_2 \cdot H_2O$			
Cu(1)–N(12)	1.9326(19)	N(12)–Cu(1)–N(18)	79.93(7)
Cu(1)–N(18)	2.0134(18)	N(12)–Cu(1)–N(1)	79.80(7)
Cu(1)–N(1)	2.0318(18)	N(18)–Cu(1)–N(1)	159.73(8)
Cu(1)–N(42)	2.067(2)	N(12)–Cu(1)–N(42)	146.53(9)
Cu(1)–N(31)	2.114(2)	N(18)–Cu(1)–N(42)	95.89(8)
		N(1)–Cu(1)–N(42)	101.00(8)
		N(12)–Cu(1)–N(31)	133.80(8)
		N(18)–Cu(1)–N(31)	97.82(8)
		N(1)–Cu(1)–N(31)	96.17(7)
		N(42)–Cu(1)–N(31)	79.63(9)

study aims at synthesis of copper(II) complexes with a tridentate and a bidenate ligands and assess their DNA cleaving ability as well as cytotoxicity.

2. Results and discussion

2.1. Synthesis and characterization of the complexes

Complexes [Cu(itpy)(dmp)]$(NO_3)_2$ (**1**) and [Cu(ptpy)(dmp)]$(NO_3)_2$ (**2**) were isolated from the reaction of itpy, ptpy and dmp with $Cu(NO_3)_2.3H_2O$ in methanol solution where itpy, ptpy and dmp stands for imidazole terpyridine, pyridine terpyridine and dimethyl phenanthroline. The tridentate (itpy/ptpy) ligand and bidenate (dmp) ligand forms copper(II) complexes of the type $Cu(II)N_5$. The TAU value for complexes **1** and **2** has been calculated [45]. These values have been found to be 0.33 for complex **1** and 0.63 for complex **2**, indicating that complex **1** has distorted square pyramidal geometry, whereas the geometry of complex **2** is between trigonal

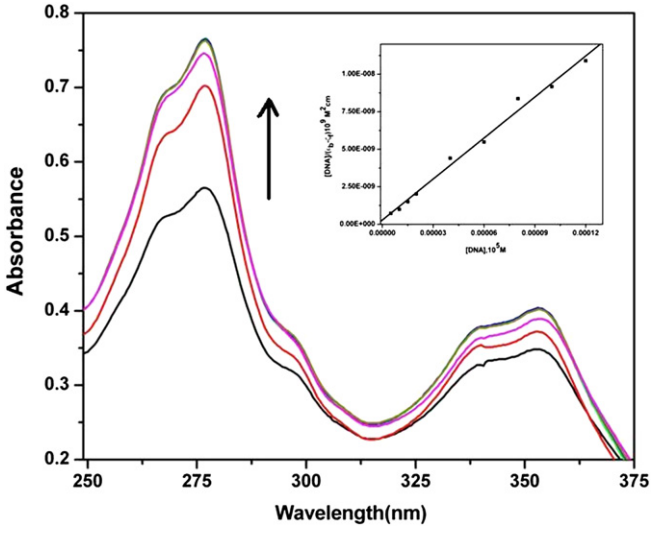

Fig. 3. Absorption spectra of complex **1** upon addition of CT-DNA. Inset: plots of [DNA]/($\varepsilon_a - \varepsilon_f$) vs. [DNA].

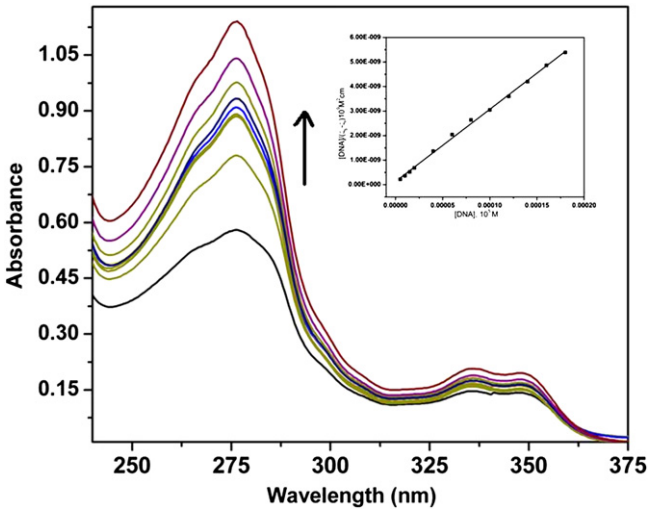

Fig. 4. Absorption spectra of complex **2** upon addition of CT-DNA. Inset: plots of [DNA]/($\varepsilon_a - \varepsilon_f$) vs. [DNA].

bipyramidal and square pyramidal. The authenticities of the complexes were confirmed by ESI-MS spectra. Electronic absorption spectra for both the complexes were recorded in acetonitrile. The UV–visible spectrum of complexes **1** and **2** are shown in Fig. 1. The spectrum of complex **1** shows strong CT band at 343 nm and intra-ligand transitions at 218 and 275 nm. The corresponding transitions for complex **2** have been observed at 350, 212 and 276 nm, respectively. The ligand field transitions have been observed as a broad band centered at 628 nm and 623 nm for complexes **1** and **2**, respectively. The cyclic voltammogram of both the complexes show irreversible cathodic wave. The Cu(II/I) reduction potential has been found to be −0.016 V vs. SCE and 0.023 V vs. SCE for complex **1** and complex **2**, respectively. The irreversible nature of the redox wave clearly shows that the reorganizational barrier during the redox process is large in both the cases.

2.2. Crystal structure

Complexes **1** and **2** were characterized structurally in a single-crystal X-ray diffraction study. The crystal structure shows the mononuclear dicationic nature of the complexes having chelating tridentate terpyridine and bidenate phenanthroline ligand derivatives. Complexes **1** and **2** crystallized with the molecular formula [Cu(itpy)(dmp)]$(NO_3)_2 \cdot 4.5H_2O$, [Cu(ptpy)(dmp)]$(NO_3)_2 \cdot H_2O$ and space groups $P2_1/c$ and $C2/c$, respectively. The ORTEP view of the complexes is shown in the Fig. 2. It depicts the coordination of the ligands as distorted square pyramidal (4 + 1) for complex **1** (Fig. 2a) and in between trigonal bipyramidal and square pyramidal for complex **2** (Fig. 2b). The basal plane of the square pyramidal complex **1** is formed by N(1), N(12) and N(18) from terpy ligand and the fourth position is occupied by N(42) from dmp ligand. The apical Cu–N(31) bond is 2.219 Å, which is slightly longer than the other Cu–N bonds. It is worthwhile to note that in the case of $[Cu(itpy)_2]^{2+}$ the axial Cu–N bond has been reported to be 2.0726 and 2.0909 Å [46]. The bipy ligand in complex **1** is roughly perpendicular to the terpy. The pyridyl rings of the dmp ligand lying on the apical position of complex **1** are π stacked with one another (see Supplementary Data). It is interesting to note that in the octahedral complex $[Cu(itpy)_2]^{2+}$, π stacking was between layered terpyridyl moieties [46]. The crystal packing clearly shows that the –NH– groups are involved in hydrogen bonding with one another (see Supplementary Data). It is interesting to observe that the imidazole

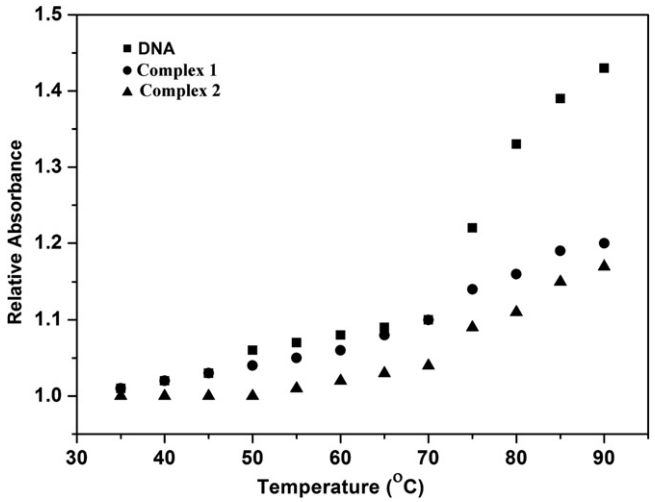

Fig. 5. Melting curves of CT-DNA upon addition of complexes **1** and **2.**

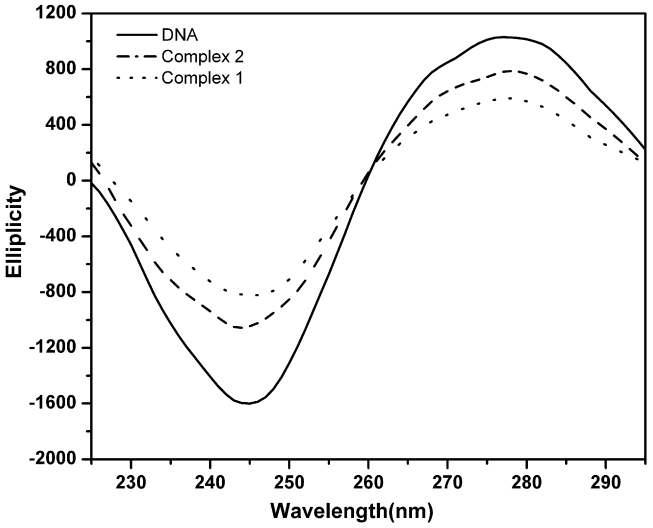

Fig. 7. Circular dichroic spectra of CT-DNA with the addition of complexes.

group containing –N– and –NH– facing outward is freely available for H-bonding (see Supplementary Data). This may have the ability to behave as H– donor and acceptor as present in the base pairs of DNA. The important bond lengths and bond angles for both the complexes are given in Table 1.

In the complex **2,** which has a structure in between trigonal bipyramidal and square pyramidal the basal plane is formed by the N(31) and N(42) from dmp ligand and N(12) of ptpy ligand. The N (1) and N(18) of terpy ligand occupies the apical position. The Cu–N (equatorial) and Cu–N (axial) distances are 2.03 Å and 2.02 Å, respectively. The pyridyl moiety in complex **2** is twisted by about 0.45°. It may be relevant to compare the Cu–N bond length of complex **2** with that of $[Cu(trien)(phen)]^{2+}$ which is reported to possess distorted square pyramidal structure. The axial Cu–N bond length in this case has been reported to be 2.186 Å which is longer than that observed for complex **2** and the equatorial Cu–N bond length ranges from 2.00 to 2.04 Å [47]. Complex **2** is an independent molecule without any π stacking and H-bonding ability. Since dmp occupies the equatorial position and both the apical positions are occupied by the aromatic pyridyl moieties, favorable π stacking may not be so facile.

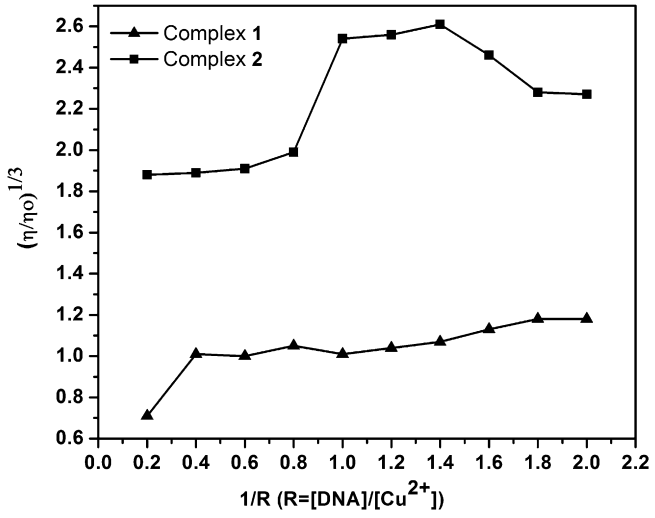

Fig. 6. Effect of complexes on the viscosity of CT-DNA.

2.3. DNA binding studies

2.3.1. Electronic spectral studies

An absorption titration method has been used to monitor the interaction of complexes **1** and **2** with Calf Thymus (CT)-DNA. The absorption spectrum of 20 μM of complexes **1** and **2** in the absence and presence of CT-DNA is shown in the Figs. 3 and 4, respectively. Binding of the complexes to DNA lead to perturbation in their ligand centered band. The absorption bands of **1** and **2** were affected with increasing concentrations of DNA. A strong hyperchromic effect in the intraligand transition was observed for complexes **1** and **2**. However, there was practically no change in the position of the absorption bands of the two complexes in the presence of DNA. These results suggest the possibility of groove binding for both the complexes to DNA. Observed spectral behavior clearly rule out intercalative binding of the complexes to DNA, since intercalation leads to hypochromism in the spectral bands [48–50]. DNA possess several hydrogen bonding sites which are accessible both in the major and minor grooves [51]. Literature reports that 2,9-disubstituted phenanthroline ring of the complexes intercalate weakly [52] and compounds with –NH– groups (from amide, benzimidazole or indole) can form hydrogen bonds with A–T base pairs. Interactions with the groove walls and phosphate groups can enhance overall complex stability [53]. The minor groove contains primarily H-bond acceptor groups, the purine N(3) and pyrimidine O(2) at the floor of the groove walls [54]. Imidazolyl group in the tridentate ligand coordinated to complex **1** contain uncoordinated –NH– group which may involve in secondary interactions like H-bonding with DNA. In order to compare quantitatively the binding affinity of complexes **1** and **2** with CT-DNA, the intrinsic binding constants K_b of the complexes were determined by monitoring the

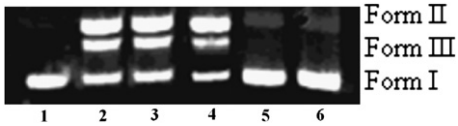

Fig. 8. Concentration dependant cleavage of SC pUC 18 DNA upon addition of complex **1**. Gel electrophoresis diagram showing the cleavage of SC pUC 18 DNA (400 ng) incubated with the complex for 60 minutes in Tris buffer (pH 7.2). Lane 1, DNA control; lane 2, DNA + 1 (40 μM); lane 3, DNA + 1 (60 μM); lane 4, DNA + 1 (80 μM); lane 5, DNA + 1 (100 μM); lane 6, DNA + 1 (120 μM).

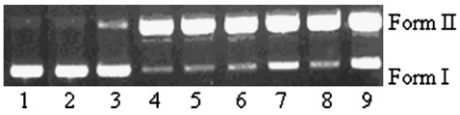

Fig. 9. Concentration dependant cleavage of SC pUC 18 DNA upon addition of complex **2** in the presence of H_2O_2. DNA (400 ng) was incubated with the complex for 60 min in Tris buffer (pH 7.2) Lane 1, DNA control; lane 2, DNA + 2 (60 μM) alone; lane 3, DNA + peroxide (1 μl) alone; lane 4, DNA + 2 (20 μM) + H_2O_2 (1 μl); lane 5, DNA + 2 (40 μM) + H_2O_2 (1 μl); lane 6, DNA + 2 (60 μM) + H_2O_2 (1 μl); lane 7, DNA + 2 (60 μM) + H_2O_2 (0.5 μl); lane 8, DNA + 2 (80 μM) + H_2O_2 (1 μl); lane 9, DNA + 2 (80 μM) + H_2O_2 (0.5 μl).

changes in absorbance of the intraligand bands with increasing concentration of CT-DNA [55]. The K_b has been calculated from equation

$$[DNA]/(\varepsilon_a - \varepsilon_f) = [DNA]/(\varepsilon_a - \varepsilon_f) + 1/K_b(\varepsilon_b - \varepsilon_f) \quad (1)$$

where ε_a, ε_f, and ε_b correspond to A_{obsd}/[Cu], the extinction coefficient for free copper complex, and the extinction coefficient for the copper complex in the fully bound form, respectively. A plot of [DNA]/($\varepsilon_a - \varepsilon_f$) vs. [DNA], gives K_b as the ratio of the slope to the intercept. The binding constants K_b of complexes **1** and **2** were determined to be $(3.3 \pm 0.32) \times 10^5$ and $(2.3 \pm 0.21) \times 10^5\ M^{-1}$, respectively. These values suggest that complex **1** has marginally stronger binding affinity for calf thymus DNA than **2**. This is not surprising since crystal structure of complex **1** show that it has H-bonding capabilities and hence may be involved in secondary H-bonding interaction with DNA.

2.3.2. Thermal denaturation and viscosity studies

Thermal denaturation studies can conveniently be used in predicting the nature of binding of the complexes to DNA and their relative binding strength [56]. A high ΔT_m value is suggestive of an intercalative mode of binding of the metal complex to DNA, while a low value (1–3 °C) indicates a non-intercalative binding mode [57]. The melting curves of CT-DNA (200 μM) in the absence and presence of both the copper complexes (20 μM) are presented in Fig. 5. T_m corresponds to the breaking of hydrogen bonds between the base pairs present in the double stranded DNA to form the single stranded DNA. With the addition of copper complexes **1** and **2**, T_m of DNA increases to 80 ± 1.5 °C at a metal complex to DNA concentration ratio of 1:10. The ΔT_m value of **1** (1 °C) and **2** (0.5 °C) suggests that these complexes bind to DNA through non-intercalative mode. To investigate further the binding nature of the complexes to DNA, viscosity measurements on the solutions of DNA incubated with the complexes have been carried out. In the viscosity measurements, the rate of flow of the buffer (10 mM Tris HCl), DNA (200 μM) and DNA with the copper complexes at various concentrations (0–160 μM) were measured. The relative specific viscosity was calculated using the equation $(t - t_o)/t_o$, where t_o is the flow time for the buffer and t is the observed flow time for DNA in the absence and presence of the complex. Data are presented as $(\eta/\eta_o)^{1/3}$ vs. $1/R$ {R = [complex]/[DNA]} where η is the viscosity of DNA in the presence of complex and η_o is the viscosity of DNA alone. The plot of relative specific viscosity $(\eta/\eta_o)^{1/3}$ vs. $1/R$ is shown in the Fig. 6. Complex **1** brings about negligible change in viscosity and **2** bring about a slight increase in viscosity of DNA on increasing the concentration of the complex. Classical intercalators like ethidium bromide (EB) cause lengthening of the DNA duplex upon the insertion of EB between the stacked bases, and this increase the relative viscosity of DNA. On the other hand, if the specific viscosity decreases, it bends or kinks the DNA helix, which is attributed to the strong covalent binding of complexes with DNA bases [58]. The results of this study clearly show the non-intercalative binding of complexes **1** and **2** to DNA.

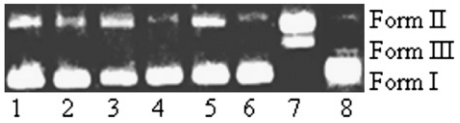

Fig. 10. Cleavage of pUC 18 DNA by complexes **1** and **2** in the presence of minor-groove binder distamycin. DNA (400 ng) was incubated with 50 μM distamycin for 15 min in Tris buffer (pH 7.2). Lane 1, DNA + distamycin (50 μM) alone; lane 2, DNA + DMSO (2 μl) alone; lane 3, DNA + peroxide (1 μl) alone; lane 4, DNA + 1 (100 μM) + distamycin (2 μl); lane 5, DNA + 1 (100 μM) + DMSO (2 μl); lane 6, DNA + 1 (100 μm); lane 7, DNA + 2(60 μM) + H_2O_2 (2 μl) + distamycin (50 μm); lane 8, DNA + 2 (60 μM) + H_2O_2 (2 μl) + DMSO (50 μm).

Table 2
MTT assay for complex **1** and complex **2**.

Concentration (μM)	Mean of % inhibition	
	Complex **1**	Complex **2**
Control	–	–
5	25.14	22.64
25	30.80	30.80
50	42.77	39.17
75	49.15	52.19
100	64.35	67.99

Data are mean percent ± SD of triplicate each.

2.3.3. Circular dichroic spectral studies

Circular dichroic studies are useful in diagnosing changes in the structure of DNA during metal complex–DNA interactions [59]. The CD spectrum of CT-DNA consists of a positive band at 284 nm due to base stacking and a negative band at 246 nm due to helicity and is characteristic of DNA in right-handed B-form [60]. On incubation with the copper complexes **1** and **2** the CD spectrum of DNA undergoes marginal changes both in its positive and negative bands (Fig. 7). In the presence of the complexes **1** and **2**, decrease in intensity of the positive band and an increase in the negative band of DNA have been observed. Both these observation clearly rule out the intercalative mode of binding of these complexes and hence suggest that the complexes bind to DNA in a non-intercalative mode. Groove binding and electrostatic interaction of the complexes with DNA has been shown to bring about only marginal changes in the intensity of negative band as well as the positive band of DNA. On the other hand intercalators are known to enhance the intensities of both these bands [61]. An increase in positive and a decrease in negative ellipticity indicate strong conformational changes [62].

2.3.4. DNA cleavage properties

The DNA strand scission chemistry of complexes has been investigated by quantification of the supercoiled (SC) form. The distribution of SC, NC (nicked circular) and linear forms of DNA in the agarose gel electrophoresis provide a measure of the extent of cleavage of DNA. Most of the copper(II) complexes bring about DNA cleavage in the presence of coreagent like ascorbate or peroxide [46]. Some complexes of copper(II) have been reported to bring about DNA cleavage even in the absence of any coreagent [41]. The hydrolytic cleavage activity of **1** has been studied using SC pUC 18 DNA in a medium of Tris HCl buffer. Complex **1** shows cleavage of SC DNA (form I) to form (II) and form (III) on 1 h incubation at 37 °C. This result suggests that the nuclease activity of complex **1** does not involve any oxidative process. Copper(II) complexes $[Cu(dmp)_2]^+$ and $[Cu(itpy)_2]^{2+}$on the other hand have been reported to be efficient cleavers of DNA under photolytic condition [63] or in the presence of reducing agents like ascorbic acid or peroxide [46]. Fig. 8 shows the effect of concentration of the complex **1** on the hydrolytic cleavage of pUC 18 DNA. The cleavage activity of the complex was assayed from the conversion of supercoiled DNA

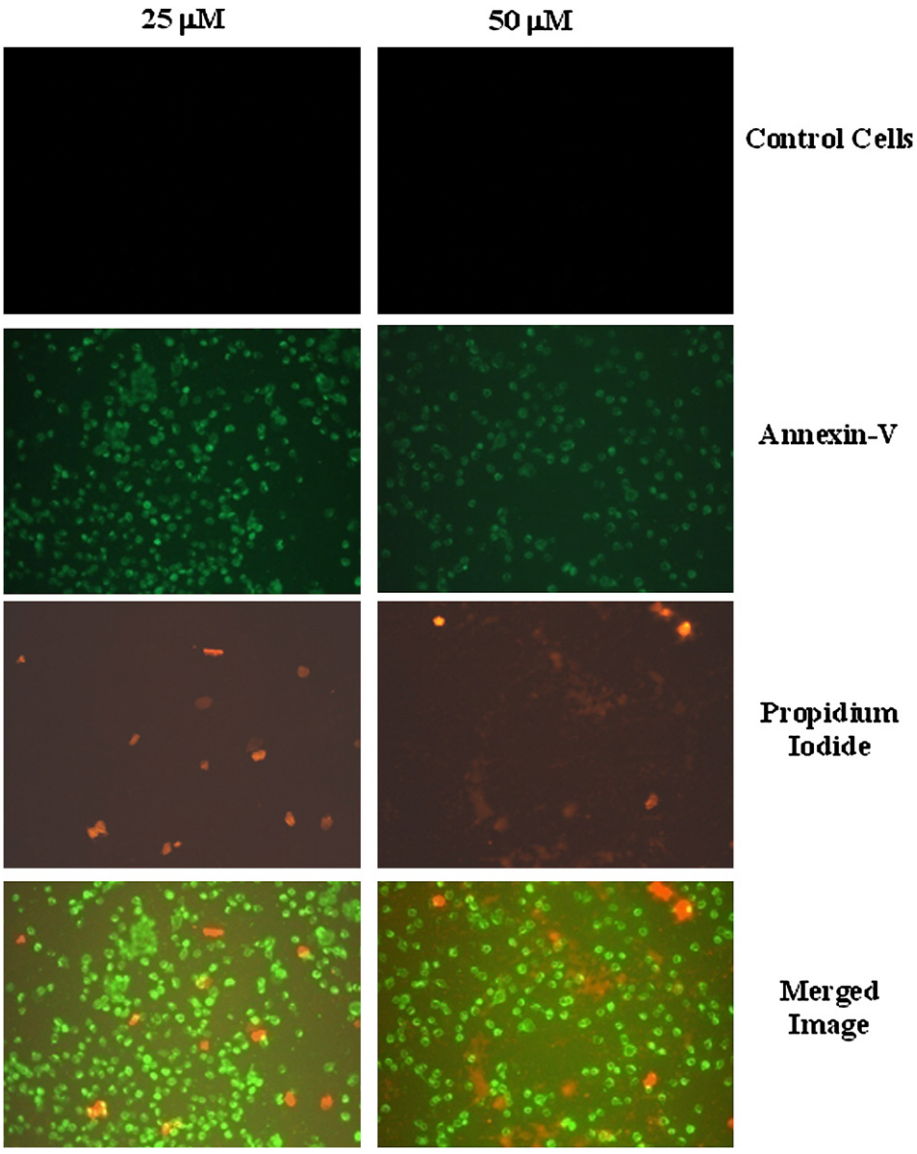

Fig. 11. Annexin-V/PI stained A-549 lung cancer cells with complex **1** and merged image.

(form I) to nicked circular DNA (form II) and linearlised DNA (form III). As can be seen from lanes 2, 3 and 4 (Fig. 8) 40, 60 and 80 μM of complex **1** was able to convert supercoiled DNA to nicked circular and linear form of DNA. Interestingly, any further increase in the concentration of complex **1** (100 and 120 μM) results in suppression of the DNA cleaving ability of the complex. It is possible that the lone pair of electrons on the imidazolyl N probably attacks the phosphodiester, resulting in the DNA cleavage. At higher concentration of the complex the imidazolyl N may be involved in H-bonding with the neighboring molecule and as a result it is not capable of initiating phosphodiester bond cleavage.

Complex **2** on the other hand does not bring about DNA cleavage in the absence of any coreagent as can be seen from Fig. 9. This complex, however, brings about DNA cleavage in the presence of H_2O_2. The control experiments performed by using complex **2** and peroxide on separate lanes reveal no cleavage of DNA as seen in lanes 2 and 3. As can be seen from lane 4, 20 μM of complex **2** was able to bring about DNA cleavage in the presence of H_2O_2. DNA cleaving experiments have also been performed in the presence of hydroxyl radical quencher, DMSO. The results show that DMSO inhibits the cleavage of DNA (Fig. 10). This clearly shows that hydroxyl radical is the reactive oxygen species for the observed cleavage in the presence of complex **2** and H_2O_2. To probe the groove binding preferences of complexes **1** and **2**, the minor-groove binder distamycin was used. Prior to the addition of complexes **1** and **2**, DNA was incubated with distamycin. The electrophoresis result (Fig. 10) shows a complete inhibition in the case of complex **1** (lane 4) while complex **2** exhibits significant DNA cleavage (lane 7). This suggests minor groove preference for the complex **1** and major groove binding for the complex **2**. Control experiments performed with SC DNA in the presence of DMSO and distamycin show absence of any significant cleavage (lanes 2 and 3). Hence, it is clear that complex **1** binds to minor groove of DNA; whereas complex **2** binds to major groove of DNA. These results are of significance as majority of the oxidative cleavage reagents generally bind in the minor groove rather than the major groove [64].

2.3.5. Cytotoxicity of the Cu(II) complexes

The cytotoxicity of complexes **1** and **2** to human lung cancer cell of A549 were measured by MTT reduction assay. The assay was based on the fact that only live cells reduce yellow MTT but not dead cells to blue formazan products. The metabolic activity of the

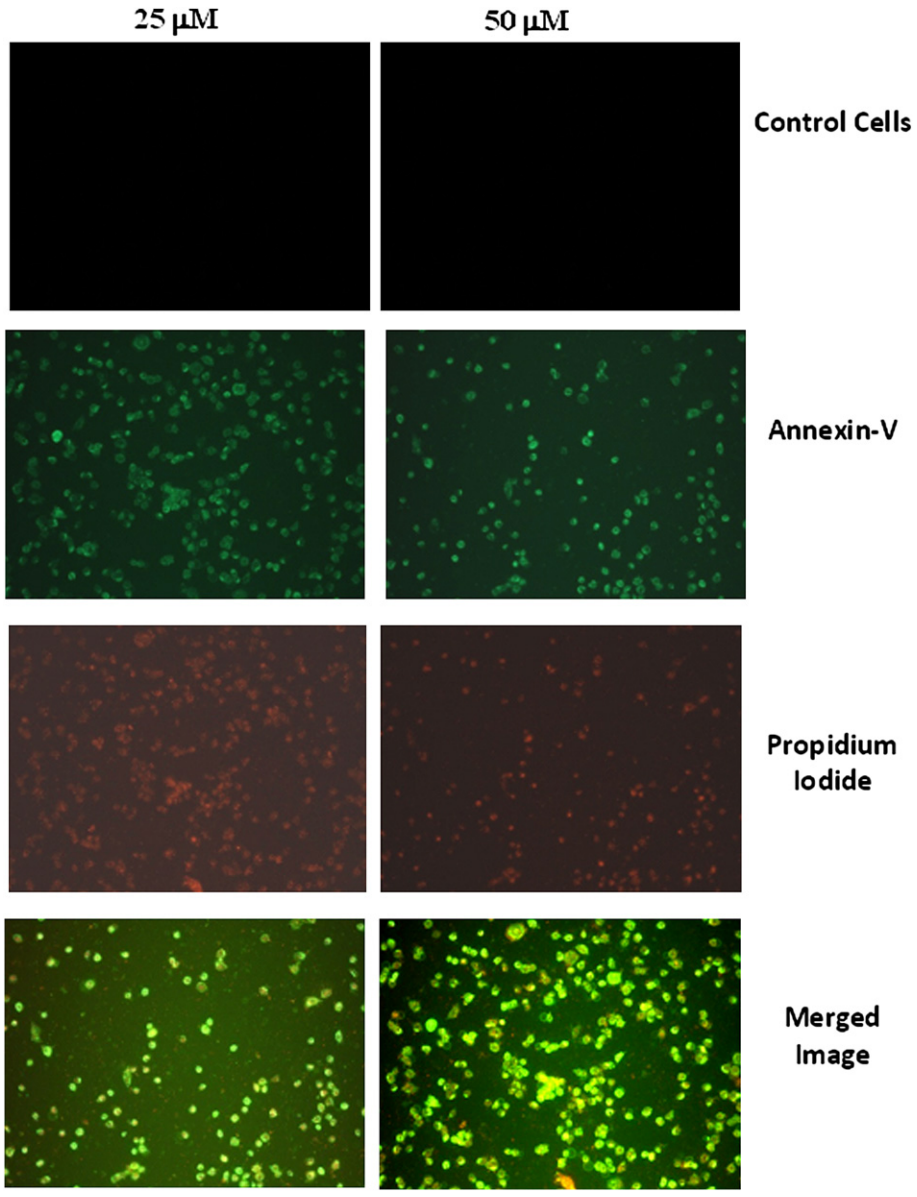

Fig. 12. Annexin-V/PI stained A-549 lung cancer cells with complex **2** and merged image.

cells was assessed by their ability to cleave the tetrazolium rings of the pale yellow MTT and form a dark blue water-insoluble formazan crystal. Results of MTT assay (Table 2) show that both the complexes inhibit the growth of the cells in a concentration dependent manner. At 100 μM concentration, complex **1** showed 64% inhibition of the cell growth, whereas complex **2** showed 68% inhibition of cell growth for the same concentration of the complex. Apoptosis is involved in the regulation of cell number in multicellular organisms and the pathogenesis of various diseases, including tumor progression, neurodegenerative disorders, and viral infections [65]. In most cell types, phosphatidylserine (PS), a lipid normally confined to the inner leaflet of the plasma membrane, is exported to the outer plasma membrane leaflet in the early stage of apoptosis. One of the early indicators of apoptosis is the rapid translocation and accumulation of the membrane phospholipid phosphatidylserine from the cell's cytoplasmic interface to the extracellular surface. This loss of membrane asymmetry can be detected using the binding properties of annexin-V [66].

In the early stages of apoptosis, the cell membrane can expose PS which is annexin-V positive [67]. Figs. 11 and 12 show the apoptotic ability of complexes **1** and **2** towards human lung tumor cells A549. A549 cells were incubated with complexes **1** and **2** for 24 h and stained with annexin-V. The stained cells were examined under a fluorescence microscope. The results show a gradient increase in the number of apoptotic cells with respect to increasing concentration of the complexes. It can be seen from Fig. 11 that complex **1** treated cells upon staining with annexin-V stain exhibit prominent green fluorescence, whereas cells treated with complex **2** exhibit relatively less green fluorescence. These results clearly show that complex **1** brings about early apoptosis to greater extent compared to complex **2**. It can also be seen from Fig. 12 that in the case of PI staining, complex **2** treated cells show more prominent orange stains compared to complex **1** treated cells. The penetration of PI inside the dead cells was evident. In contrast, the cells which were not treated with any of the complexes, demonstrated normal cell viability with no remarkable cell death. It is indeed noteworthy

that both the complexes show different cytotoxic pathway, complex **1** is able to induce early apoptosis and complex **2** brings about late apoptosis towards human lung tumor cells.

3. Conclusion

Two mixed ligand copper(II) complexes of tridentate ligands itpy and ptpy along with the bidentate ligand dmp namely [Cu(itpy)(dmp)]$(NO_3)_2$ (**1**) and [Cu(ptpy)(dmp)]$(NO_3)_2$ (**2**) have been synthesized and crystallographically characterized. Complex **1** has been found to possess square pyramidal geometry, while the complex **2** geometry has been found to be between trigonal bipyramidal and square pyramidal. DNA binding studies reveal that both the complexes prefer groove binding; complex **1** binding to the minor groove and complex **2** binding to the major groove of DNA. Both the complexes have been found to promote DNA cleavage. However, the mechanism of DNA cleavage promoted by the two complexes is different. While complex **1** was able to bring about hydrolytic cleavage of DNA, complex **2** was unable to do so. However, complex **2** brought about oxidative cleavage of DNA. Complex **1,** which brought about hydrolytic cleavage of DNA induced early apoptosis to A549 cells whereas complex **2** which requires external additive for DNA cleavage induced late apoptosis. These results clearly show that both the complexes possess anti-tumor activity.

4. Experimental

4.1. Materials

2-Acetyl pyridine, 2,9-dimethyl phenanthroline, 2-imidazole carbaldehyde, pyridine-4-carbaldehyde, calf thymus DNA, agarose, ethidium bromide and annexin-V-FITC staining kit were obtained from Sigma Aldrich. Tris (hydroxymethyl) methylamine and TBE was obtained from SRL chemicals, Mumbai.

4.2. Instrumentation

Electronic spectra were recorded using a Perkin–Elmer Lambda 35 double beam spectrophotometer. The C, H and N microanalyses were done using a Eurovector CHNS elemental analyzer. Electrospray ionization mass spectra (ESI-MS) were obtained from Thermo Finnigan LCQ 6000 advantage max ion trap mass spectrometer using acetonitrile as carrier solvent. Cyclic voltammetry experiments were conducted on a CH instrument (USA) model CH-620B electrochemical analyzer. The electrochemical workstation was equipped with three electrode system namely, glassy carbon working electrode, a platinum wire auxiliary electrode and a saturated calomel reference electrode. All the redox potential values reported are with respect to SCE. Tetrabutyl ammonium perchlorate was used as supporting electrolyte for the electrochemical work. Nitrogen gas was purged prior to all the measurements. For apoptotic assessment, the fluorescence was measured by inverted fluorescent microscope (Nikon, Japan).

A stock solution of DNA was prepared by stirring a sample dissolved in 10 mM Tris HCl buffer (pH 7.2) at 4 °C and used within 4 days. The solution was dialysed exhaustively against Tris buffer for 48 h and filtered using a membrane filter obtained from sartorius (0.45 μM). The filtered DNA solution in the buffer gave a UV absorbance ratio (A_{260}/A_{280}) of about 1.9, indicating that the DNA was sufficiently free from protein [68]. The concentration of DNA was determined using an extinction coefficient of 6600 $M^{-1}\,cm^{-1}$ at 260 nm [69]. All the experiments were carried out in Tris buffer at pH 7.2 in Mill − Q triply deionized water.

4.3. Synthesis of ligands, complexes 1 and 2

The ligands (itpy and ptpy) were synthesized as reported in literature [70]. The complex **1** was prepared by stirring a methanolic solution of $Cu(NO_3)_2\cdot 3H_2O$ (0.12 g, 0.5 mmol) with itpy (0.15 g, 0.5 mmol) under room temperature for 15 min. Subsequently to the above solution dmp (0.12 g, 0.5 mmol) was added and continued stirring for another 15 min. The reaction mixture was then set aside for slow evaporation. A green solid that separated out upon slow evaporation of the solvent was filtered, and washed with diethyl ether and dried in vacuum. The complex [Cu(Itpy)(dmp)]$(NO_3)_2$ was recrystallized from acetonitrile. Yield: 79%. Found C, 50.03; H, 4.46; Cu, 8.27; N, 16.41. Anal. Calcd. For $C_{32}H_{27}CuN_7$: C, 49.97; H, 4.05; Cu, 8.09; N, 15.11%. ESI-MS *m/z* 285, $[Cu(itpy)(dmp)]^{2+}$. Single crystals which are suitable for X-ray diffraction studies were obtained upon slow evaporation of the solvent.

The complex **2** was synthesized employing the same procedure as said above with ptpy (0.31 g, 1 mmol), dmp (0.21 g, 1 mmol) and $Cu(NO_3)_2\cdot 3H_2O$ (0.24 g, 1 mmol). Yield: 76%. Found: C, 69.82; H, 4.56; N, 13.83; Cu, 10.51. Anal. Calcd. For $C_{34}H_{28}CuN_6$: C, 69.90; H, 4.83; N, 14.39; Cu, 10.88%. ESI-MS *m/z* 291, $[Cu(ptpy)(dmp)]^{2+}$. The green precipitate obtained was dissolved in acetonitrile–water mixture and kept for volatilizing the solvent at room temperature. After several days, crystals suitable for X-ray diffraction analysis were obtained.

4.4. X-ray crystallographic data collection and refinement of the structures

Green single crystals of [Cu(itpy)(dmp)]$(NO_3)_2\cdot 4.5H_2O$ and [Cu(ptpy)(dmp)]$(NO_3)_2\cdot H_2O$ were coated with perfluoropolyether and mounted in the nitrogen cold stream (100 K) of the diffractometer equipped with a Mo-target rotating-anode X-ray source (Mo-Kα, $\lambda = 0.71073$ Å). Final cell constants were obtained from least squares fits of several thousand strong reflections. Crystallographic data of the compounds are listed in Table 3. The Siemens ShelXTL [71] software package was used for solution and artwork of the structure ShelXL97 [72] was used for the refinement. The structure was readily solved by Patterson method and subsequent difference Fourier techniques. All non-hydrogen atoms were anisotropically refined. Hydrogen atoms attached to carbon atoms were placed at

Table 3
Crystallographic data for complex **1** and complex **2**.

Parameters	Complex **1**	Complex **2**
Chemical formula	$C_{32}H_{34}CuN_9O_{10.5}$	$C_{34}H_{30}CuN_8O_8$
Fw	776.22	742.20
Space group	$P2_1/c$, No. 14	$C2/c$, No. 15
a, Å	17.924(2)	45.785(9)
b, Å	19.100(3)	7.5986(14)
c, Å	19.908(2)	18.192(4)
β, deg	96.411(8)	91.800(4)
V, Å	6772.9(15)	6326(2)
Z	8	8
T, K	100(2)	100(2)
ρ calcd, g cm^{-3}	1.522	1.559
Reflections collected/$2\Theta_{max}$	130,298/60.00	84,425/61.00
Unique reflections/$I > 2\sigma(I)$	19,729/14,964	9622/6969
No. of parameters/restraints	1044/325	462/0
μ, cm^{-1}/λ, Å	7.19/0.71073	7.60/0.71073
R_1[a]/goodness of fit[b]	0.0604/1.104	0.0475/1.020
wR_2[c] ($I > 2\sigma$ (I))	0.1323	0.1180
Residual density, eÅ^{-3}	+0.93/−0.85	+0.90/−0.98

[a] Observation criterion: $I > 2\sigma(I)$. $R1 = \Sigma||F_o| - |F_c||/\Sigma|F_o|$.
[b] $GooF = [\Sigma[w(F_o^2 - F_c^2)^2]/(n-p)]^{1/2}$.
[c] $wR_2 = [\Sigma[w(F_o^2 - F_c^2)^2]/\Sigma[w(F_o^2)^2]]^{1/2}$ where $w = 1/\sigma^2(F_o^2) + (aP)^2 + bP, P = (F_o^2 + 2F_c^2)/3$.

calculated positions and refined as riding atoms with isotropic displacement parameters. Hydrogen atoms of solvent water molecules and hydrogen atoms bound to nitrogen atoms were localized from the difference map and were refined with restrained O–H distances and displacement parameters.

A nitrate anion and a water molecule in [Cu(itpy)(dmp)] $(NO_3)_2 \cdot 4.5H_2O$ were found to be severely disordered. An initial attempt to model the disorder of the anion with two split positions was not satisfying. Finally a model with three split positions for the nitrate anion was chosen. DFIX, SADI and EADP instructions of ShelXL97 were used to restrain bond distances, angles and thermal displacement parameters. The occupation factors refined to values of about 0.49, 0.39, 0.12 for the split positions containing N(500), N (510), N(520), respectively. Only two positions of the water molecule forming hydrogen bonds to the nitrate ion and other water molecules could be identified. The occupation ratio refined to 0.65:0.35 (O(670) and O(675)). The CCDC deposition numbers for complex **1** and complex **2** are 781794 and 781795 respectively.

4.5. DNA binding and cleavage experiments

Concentrated stock solutions of metal complexes were prepared by dissolving the complexes in acetonitrile and diluting suitably with 10 mM Tris [tris(hydroxyl methyl) methylamine] HCl at pH 7.2 (1:10 as acetonitrile: buffer) to required concentration for all the experiments. Absorption spectral titration experiments were carried out by monitoring the electronic spectrum of 20 μM of the complex in the presence of varying CT-DNA concentration (0–160 μM).

For viscosity measurements, the Ubberhold viscometer (1 mL capacity) was thermostated in waterbath maintained at 25 °C. The flow time for each sample was measured three times using digital stopwatch and an average flow time was calculated. The rate of flow for the buffer (10 mM Tris), DNA (100 μM) and DNA with the copper complexes at various concentrations (0–200 μM) were measured. The relative specific viscosity was calculated using the equation $\eta = (t - t_o)/t_o$, where t_o is the flow time for the buffer and t is the observed flow time for DNA in the absence and presence of complex. Data are presented as $(\eta/\eta_o)^{1/3}$ vs. $1/R$ $\{R = [\text{complex}]/[\text{DNA}]\}$ where η is the viscosity of DNA in the presence of complex and η_o is the viscosity of DNA alone [73]. Thermal denaturation experiments were carried out with the Perkin–Elmer Lambda 35 spectrophotometer equipped with a Peltier temperature-control programmer. The temperature was gradually increased from 25 °C to 95 °C at a rate of 3 °C min^{-1}. The absorbance at 260 nm was recorded for CT-DNA (200 μM) in the absence and presence of both the copper(II) complexes (20 μM) at an interval of 5 °C. The T_m values were determined from the plot of relative absorbance $(A \cdot A_{25}^{-1})$ vs. temperature, where A is the observed absorbance and A_{25} is the absorbance at 25 °C.

Circular dichroic spectra were recorded with a Jasco J-715 spectropolarimeter at 25 °C using 0.1 cm quartz cell. The concentration of CT-DNA (100 μM) was kept constant and the concentration of copper complexes **1** and **2** varied from 10 to 40 μM.

Cleavage of DNA by copper (II) complexes was monitored by using the agarose gel electrophoresis technique. The DNA cleavage efficiency of complexes **1** and **2** was monitored by determining their ability to convert supercoiled DNA (Form I) to open circular (Form II) and linear forms (Form III). The cleavage experiments were carried out in the absence and presence of any activating agents. The samples were incubated for 1 h at 37 °C. In the inhibition reactions, additives like distamycin or DMSO were added to the supercoiled DNA and the incubation carried out for 15 min at 37 °C prior to the addition of the complex and peroxide. To identify the reactive oxygen species (ROS) involved in the cleavage reaction, we introduced the radical scavenger DMSO. A loading buffer containing 0.25% bromophenol blue, 40% (w/v) sucrose and 0.5 M EDTA was added and the electrophoresis of the DNA cleavage products were performed on agarose gel containing ethidium bromide. The gels were run at 50 V for 2 h in Tris-boric acid–ethylenediamine tetra acetic acid (TBE) buffer at pH 7.4. The cleavage of DNA was monitored using 0.8% agarose gel electrophoresis containing 0.5 μg/mL ethidium bromide. The bands were viewed by placing the gel on UV illuminator and were photographed using gel documentation system.

4.6. Determination of cytotoxicity on cancer cell lines

Proliferation of A549 lung adenocarcinoma cells was assessed by 3-(4,5-dimethylthiazol-2-yl)-2,5-diphenyltetrazolium bromide (MTT) dye assay [74]. Cells were plated in 96-well plates at a concentration of 5×10^4 cells/well. After 24 h the plates were washed twice with 200 μl of serum-free medium and were starved by incubation in serum-free medium for 1 h at 37 °C. After starvation, cells were treated with aqueous solutions of the copper complexes of different concentrations for 24 h. At the end of the treatment, media from control and complex-treated cells were discarded and 20 μl of MTT-containing DMEM (0.5 mg/ml) was added to each well. Cells were then incubated for 4 h at 37 °C in a CO_2 incubator. MTT-containing medium was then discarded and the cells were washed with 1× phosphate-buffered saline (PBS; 1 ml). Coloured metabolite was then dissolved by adding 180 μl of DMSO solution and this was mixed effectively by pipetting up and down. Spectrophotometrical absorbance of the purple blue formazan dye was measured using an ELISA reader at 620 nm.

To detect apoptosis, annexin-V antibody conjugated with the fluorescent dye fluorescein isothiocyanate was employed. The kit uses a staining protocol in which the early apoptotic cells are stained with annexin-V (green fluorescence) with the excitation wavelength (λ_{ex}) 488 nm and emission wavelength (λ_{em}) 520 nm. Late apoptotic cells are stained with Propidium iodide (red fluorescence) with λ_{ex} 540 nm and λ_{em} 630 nm. Viable cells are neither stained by annexin-V nor propidium iodide. The A549 lung adenocarcinoma cells were grown to 70% confluency and treated with complexes **1** and **2** for 24 h. Cells that bound FITC-annexin-V but excluded propidium iodide are termed early apoptotic cells and permeant to propidium iodide in spite of whether or not they bound FITC-annexin-V are deemed late apoptotic. Cells were counted regardless of morphology. For each sample, at least 300 cells/well were counted, and the percentage of apoptotic cells was determined using equation.

$$\%\,\text{of apoptotic cells} = (\text{total number of apoptotic cells}) / (\text{total number of cells counted}) \times 100$$

The results were expressed in terms of mean ± SD.

Acknowledgement

One of the authors (SR) wishes to thank CSIR for the Junior Research Fellowship. SR thanks Manikandamathavan for his help and support.

Appendix A. Supplementary data

Supplementary data associated with this article can be found, in the online version, at doi:10.1016/j.ejmech.2010.11.041.

References

[1] K.H. Thompson, C. Orvig, Dalton Trans. (2006) 761–764.
[2] I. Kostova, Curr. Med. Chem. 13 (2006) 1085–1107.
[3] K.H. Thompson, C. Orvig, Science 300 (2003) 936–939.
[4] Y. Chen, Y.J. Liu, Q. Li, K.Z. Wang, J. Inorg. Biochem. 103 (2009) 1395–1404.

[5] H.T. Chifotides, K.R. Dunbar, Acc. Chem. Res. 38 (2005) 146–156.
[6] H. Xu, Y. Liang, P. Zhang, F. Du, B.R. Hou, J. Wu, J.H. Liu, J. Biol. Inorg. Chem. 10 (2005) 529–538.
[7] V. Brabec, Nucleic Acid Res. Mol. Biol. 71 (2002) 1–68.
[8] J. Reedijk, Proc. Natl. Acad. Sci. U S A 7 (2003) 3611–3616.
[9] T.W. Hambley, Dalton Trans. (2007) 4929–4937.
[10] H.J. Yu, S.M. Huang, L.Y. Li, H.N. Jia, H. Chao, Z.W. Mao, J.Z. Liu, N. Ji, J. Inorg. Biochem. (2009) 881–890.
[11] V.G. Vaidyanathan, B.U. Nair, J. Inorg. Biochem. 95 (2003) 334–342.
[12] Y. Sun, S.N. Collins, L.E. Joyce, C. Turro, Inorg. Chem. 49 (2010) 4257–4262.
[13] V.G. Vaidyanathan, B.U. Nair, Dalton Trans. (2005) 2842–2848.
[14] V. Uma, A. Castineiras, B.U. Nair, Polyhedron 26 (2007) 3008–3016.
[15] V.G. Vaidyanathan, B.U. Nair, Eur. J. Inorg. Chem. (2003) 3633–3638.
[16] R. Indumathy, T. Weyhermuller, B.U. Nair, Dalton Trans. (2010) 2087–2097.
[17] H. Prakash, A. Shodal, H. Yasul, H. Sakural, S. Hirota, Inorg. Chem. 47 (2008) 5045–5047.
[18] M.S.S. Babu, K.H. Reddy, P.G. Krishna, Polyhedron 26 (2007) 572–580.
[19] S. Delaney, M. Pasclay, P.K. Bhattacharya, K. Han, J.K. Barton, Inorg. Chem. 41 (2002) 1966–1974.
[20] T.K. Goswami, M. Roy, M. Nethaji, A.R. Chakravarty, Organometallics 28 (2009) 1992–1994.
[21] B. Macias, M.V. Villa, F. Sanz, J. Borras, M.G. Alvarez, G. Alzuet, J. Inorg. Biochem. 99 (2005) 1441–1448.
[22] V. Uma, V.G. Vaidyanathan, B.U. Nair, J. Bull. Chem. Soc. Jpn. 78 (2005) 845–850.
[23] V.G. Vaidyanathan, B.U. Nair, J. Inorg. Biochem. 93 (2003) 271–276.
[24] M.D. Kuwabara, C. Yoon, T.E. Goyne, T. Thederahn, D.S. Sigman, Biochemistry 25 (1986) 7401–7408.
[25] G. Sathyaraj, T. Weyhermuller, B.U. Nair, Eur. J. Med. Chem. 45 (2010) 284–291.
[26] P.K. Sasmal, R. Majumdar, R.R. Dighe, A.R. Chakravarty, Dalton Trans. 39 (2010) 104–7113.
[27] H.J. Yu, S.M. Huang, L.Y. Li, H.N. Jia, H. Chao, Z. Wan, J.Z. Liu, L.N. Ji, J. Inorg. Biochem. 103 (2009) 881–890.
[28] A.K. Patra, T. Bhowmick, S. Roy, S.R. Ramakumar, A.R. Chakravarty, Inorg. Chem. 48 (2009) 2932–2943.
[29] Q.L. Zhang, J.G. Liu, H. Chao, G.Q. Xue, L.N. Ji, J. Inorg. Biochem. 83 (2001) 49–58.
[30] V.G. Vaidyanathan, B.U. Nair, Eur. J. Inorg. Chem. (2004) 1840–1846.
[31] B. Zhu, D.Q. Zhao, J.Z. Ni, Q.H. Zeng, B.Q. Huang, Z.L. Wang, Chem. Commun. 2 (1999) 351–353.
[32] D.A. Knight, J.B. Delehanty, E.R. Goldman, J. Chang, Dalton Trans. (2004) 2006–2011.
[33] C. Sissi, P. Rossi, F. Felluga, F. Formaggio, M. Palumbo, P. Teccilla, C. Toniolo, P. Scrimin, J. Am. Chem. Soc. 123 (2001) 3169–3170.
[34] M.E. Branum, L. Que Jr., J. Biol. Inorg. Chem. 4 (1999) 593–600.
[35] C. Sissi, F. Mancin, M. Gatos, M. Palumbo, P. Teccilla, U. Tonellato, Inorg. Chem. 44 (2005) 2310–2317.
[36] C. Liu, S. Yu, D. Li, Z. Liao, X. Sun, H. Xu, Inorg. Chem. 41 (2002) 913–922.
[37] J.A. Cowan, Chem. Rev. 98 (1998) 1067–1088.
[38] A. Sreedhara, J.A. Cowan, J. Biol, Inorg. Chem. 6 (2001) 337–347.
[39] B. Meunier, Chem. Rev. 92 (1992) 1411–1456.
[40] E.L. Hegg, J.N. Burstyn, Coord. Chem. Rev. 173 (1998) 133–165.
[41] S. Dhar, P.A.N. Reddy, A.R. Chakravarty, Dalton Trans. (2004) 697–698.
[42] T. Gupta, S. Dhar, M. Nethaji, A.R. Chakravarty, Dalton Trans. (2004) 1896–1900.
[43] P.U. Maheshwari, S. Roy, H.D. Dulk, S. Barendes, G.V. Wezel, B. Kozlevkar, P. Gamez, J. Reedjik, J. Am. Chem. Soc. 128 (2006) 710–711.
[44] P.U. Maheshwari, M.V.D. Ster, S. Smulders, S. Barendes, G.P.V. Wezel, C. Massera, S. Roy, H.D. Dulk, P. Gamez, J. Reedjik, Inorg. Chem. 47 (2008) 3719–3727.
[45] A.W. Addision, T.N. Rao, J. Reedijk, J. van Riju, G.C. Verschoor, J. Chem. Soc., Dalton Trans. (1984) 1349–1356.
[46] V. Uma, M. Kanthimathi, T. Weyhermuller, B.U. Nair, J. Inorg. Biochem. 99 (2005) 2299–2307.
[47] R.N. Patel, N. Singh, K.K. Shula, J.N. Gutierrez, A. Castineiras, V.G. Vaidayanathan, B.U. Nair, Spectrochim. Acta A 62 (2005) 261–268.
[48] G.Y. Bai, B. Dong, Y.Y. Lu, K.Z. Wang, L.P. Jin, L.H. Gao, J. Inorg. Biochem. 98 (2004) 2011–2015.
[49] X.L. Wang, H. Chao, H. Li, X.L. Hong, Y.J. Liu, L.F. Tan, L.N. Ji, J. Inorg. Biochem. 98 (2004) 1143–1150.
[50] J.K. Barton, A.T. Danishefsky, J.M. Goldberg, J. Am. Chem. Soc. 106 (1984) 2172–2176.
[51] H.L. Chan, Q.L. Liu, B.C. Tzeng, Y.S. You, S.M. Peng, M. Yang, C.M. Che, Inorg. Chem. 41 (2002) 3161–3171.
[52] P. Zhang, J. Chen, Y. Liang, Acta Biochim. Biophys. Sin. 42 (2010) 440–449.
[53] B. Nguyen, S. Neidle, W. David, Chem. Res. 42 (2009) 11–21.
[54] S. Neidle, Nat. Prod. Rep. 18 (2001) 291–309.
[55] A.M. Pyle, J.P. Rehmann, R. Meshoyrer, C.V. Kumar, N.J. Turro, J.K. Barton, J. Am. Chem. Soc. 111 (1989) 3051–3058.
[56] S.D. Choi, M.S. Kim, S.K. Kim, P. Lincoln, E. Tuite, B. Norden, Biochemistry 36 (1997) 214–223.
[57] M. Cory, D.D. Mckee, J. Kagan, D.W. Henry, J.A. Miller, J. Am. Chem. Soc. 107 (1985) 2528–2536.
[58] P.U. Maheswari, M. Palaniandavar, J. Inorg. Biochem. 98 (2004) 219–230.
[59] A.M. Polyanichko, V.V. Andrushchenko, E.V. Chikhirzhina, V. Vorobev, H. Wieser, Nucleic Acids Res. 32 (2004) 989–996.
[60] V.I. Ivanov, L.E. Minchenkova, A.K. Schyolkina, A.I. Poletayer, Biopolymers 12 (1973) 89–110.
[61] K. Karidi, A. Garoufis, A. Tsipis, N. Hadjiliadis, H.D. Dulk, J. Reedijk, Dalton Trans. (2005) 1176–1187.
[62] P. Tamilselvi, M. Palaniandavar, Inorg. Chim. Acta 337 (2002) 420–428.
[63] D.R. McMillin, M.T. Buckner, B.T. Ahn, Inorg. Chem. 6 (1977) 943–945.
[64] W.K. Pogozelski, T.D. Tullius, Chem. Rev. 98 (1998) 1089–1107.
[65] H. Steller, Science 267 (1995) 1445–1449.
[66] S.J. Martin, C.P. Reutelingsperger, A.J. McGahon, J.A. Rader, R.C.V. Schie, D.M. LaFace, D.R. Green, J. Exp. Med. 182 (1995) 1545–1556.
[67] C. Riccardi, I. Nicoletti, Nat. Protoc. 1 (2006) 1458–1461.
[68] J. Marmur, J. Mol. Biol. 3 (1961) 208–218.
[69] M.F. Reichman, S.A. Rice, C.A. Thomas, P. Doty, J. Am. Chem. Soc. 76 (1954) 3047–3053.
[70] G.W.V. Care, C.L. Raston, J. Chem. Soc., Perkin Trans. 1 (2001) 3258–3264.
[71] ShelXtl V. 6.12. Bruker AXS, 2001.
[72] G.M. Sheldrick, ShelXL97. University of Gottingen, 1997.
[73] B. Chaires, N. Dattaguota, D.M. Crothers, Biochemistry 21 (1982) 3933–3940.
[74] F.F. Safadi, J. Xu, S.L. Smock, R.A. Kanaan, A.H. Selim, P.R. Odgren, S.C. Marks Jr., T.A. Owen, S.N. Popoff, J. Cell. Physiol. 196 (2003) 51–62.